Effects of Carbon Fiber/Al Interface on Mechanical Properties of Carbon-Fiber-Reinforced Aluminum-Matrix Composites

SHENG-HAN LI and CHUEN-GUANG CHAO

Carbon-fiber (CF)–reinforced aluminum-matrix composites were prepared by spreading fibers and squeeze casting. The interface structure of CF/Al composites was examined using high-resolution transmission electron microscopy (HRTEM) and electron spectroscopy for chemical analysis (ESCA). Aluminum carbide (Al_4C_3) interfacial reaction products were observed to nucleate heterogeneously from carbon fibers and to grow toward the aluminum matrix in the form of lath-like crystals after heat treatment. The growth of aluminum carbide was anisotropic, since it was faster along the *a*- and *b*-axes of the basal plane than along the *c*-axis. Both the tensile strength and the elongation of composites decline with an increased duration of heat treatment. The results of ESCA revealed that approximately 1 pct of carbide enhanced interface bonding. However, increasing the content of brittle carbides to over 3 pct after heat treatment degraded the mechanical properties of composites.

I. INTRODUCTION

OVER the years, carbon fibers have been considered as very important reinforcements for aluminum and its alloys in fabricating advanced composite materials. Carbon fiber (CF) reinforcement/aluminum-matrix composites are of great interest because of their high specific strength and stiffness, low coefficient of thermal expansion, and high thermal/electrical conductivity.[1–5] Consequently, CF/Al composites have the most potential to be applied as structural and functional materials in the future. The main problems encountered in the development of CF/Al composites are the reactivity of carbon with aluminum and the poor wetting characteristics of carbon by liquid aluminum.

The carbon-aluminum interface importantly affects a crucial role in the overall performance of composite materials. Improper wetting and chemical reactions at the interface during synthesis or under service conditions can degrade the mechanical properties of the composites.[3–11] The reaction at the carbon-aluminum interface at temperatures above 500 °C to form aluminum carbide (Al_4C_3) has long been considered to affect critically the strength of C/Al composites.[12,13,14] However, although many studies have been performed to evaluate the effect of reaction products on C/Al composites, their conclusions contradict each other.[15–18] Blankenburgs[16] showed that aluminum carbide formed on the surface of carbon fibers at temperatures above 500 °C. The tensile strength of the composite improved considerably after small amounts of carbide were generated. However, further growth of the carbide phase did not reduce the strength of the composite. In contrast, Khan[15] demonstrated that up to 500 °C, the strength was only slightly degraded, while for composites exposed to higher temperatures, the strength declined quite considerably. The formation of aluminum carbide at the fiber-matrix interface

was also considered to induce poor composite properties, as observed by Pepper and Penty[19] and Xiangun and Hanlin.[20] Khan[15] considered diffusion bonding by depositing films of aluminum onto carbon substrates and reported that the carbide grew as single crystals perpendicular to the c-axis of the lattice. Other researchers[21,22] conducted similar experiments and verified that the carbide growth is a diffusion-controlled process. Yang *et al*.[23] examined the growth patterns of the aluminum carbide in C/Al composites. They suggested that two kinds of interfaces exist between the carbide and aluminum matrix. They have different growth mechanisms and growth rates, given their different driving forces for growth. Several crystal relative orientations between the carbide and the aluminum matrix have been observed. The apparent inconsistency between the results is attributable, to some extent, to the presence of various fibers and/or processing methods. Further work is clearly required to help resolve the issue.

This study addresses the microstructure of the interface and the growth mechanism of the carbide in a CF/AI composite using a number of techniques, including high-resolution transmission electron microscopy (HRTEM), electron spectroscopy for chemical analysis (ESCA), and scanning electron microscopy (SEM). Additionally, the relationship between the mechanical properties and the amounts of carbide is also considered.

II. EXPERIMENTAL

The investigated composites were fabricated by squeeze casting. First, preforms were made using tows of 12,000 polyacrylontrile (PAN) carbon fibers. Then, composites were fabricated with 14 vol pct of unidirectional reinforcing fibers. The fabrication of preforms was described in the authors' earlier work.[24] In squeeze casting, the temperatures of the preform and the molten Al were 500 °C and 800 °C, respectively, at an in-filtration pressure of 36 MPa. The pressure was maintained for 90 seconds. Specimens were heat treated at 600 °C with heating rates of 3 °C/min for 12, 36, and 60 hours, respectively. Dry nitrogen gas was purged into the furnace to prevent oxidation.

SHENG-HAN LI, formerly Graduate Student, is a Ph.D. Candidate at the Dept. of Materials Science and Engineering, University of California, Los Angeles and CHUEN-GUANG CHAO, Professor, are with the Department of Materials Science and Engineering, National Chaio Tung University, Taiwan 30049, Republic of China. Contact: c_g_chao@hotmail.com
Manuscript submitted May 7, 2002.

Carbon fibers were extracted from CF/Al composites using 2 N HCl solutions. The fibers were observed by SEM. The interfaces in these composites were investigated with HRTEM (JEOL* 2010F). Specimens of HRTEM were

---

*JEOL is a trademark of Japan Electron Optics Ltd., Tokyo.

---

mechanically polished to 20 to 40 μm and then ion thinned at an accelerating voltage of 5 kV and angle of 13 deg with a liquid nitrogen cold stage. The ESCA measurements involve recording the intensity of emitted electrons as a function of the electron binding energy. The measured spectra show peaks at characteristic energies, from which the elemental composition of the fiber can be determined. The fiber surface was also analyzed using a Physical Electronics ESCA PHI 1600 apparatus, with monochromatic Al K_α radiation.

After heat treatment, tensile specimens were machined to a gage length of 16.6 mm with a cross section of 4.2×3.0 mm. Tensile tests were performed at room temperature in an Instron 4410 testing machine at a crosshead speed of 0.5 mm/min. The SEM revealed the fracture surfaces of the material.

III. RESULTS

A. Surface Morphologies

Figure 1(a) depicts the surface of an original fiber. The surface is very smooth, without any defects. Figures 1(b) through (d) illustrate the scanning electron micrographs of fibers extracted from the heat-treated composites for various periods (12, 36, and 60 hours) at 600 °C. A small amount of product was found on the surface of the heat-treated specimens. The amount and the size of the products increase with the duration of heat treatment.

B. Interface between the Carbide and the Matrix

The TEM analysis, as shown in Figure 2, revealed the little product at the interface of the as-cast CF/Al composites to be Al_4C_3. A particle was identified as a single crystal, which nucleated discontinuously at the fiber surface and grew into the molten matrix in a variety of directions. Figures 2(b) and (c) present a tilting sequence of selected-area diffraction (SAD) patterns around a row of the closest diffraction spots. The patterns are indexed according to the rhombohedral structure of the carbide phase, Al_4C_3, with a space group of R3m and
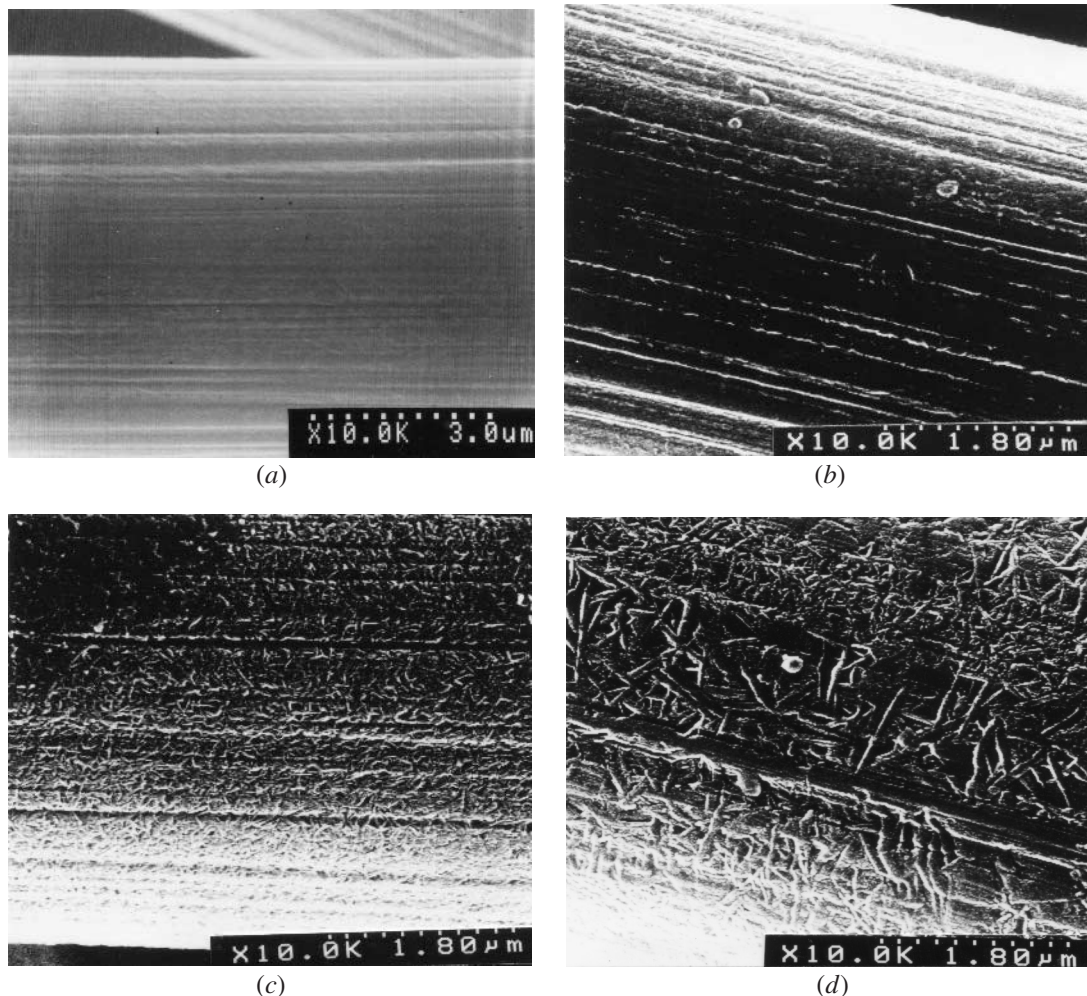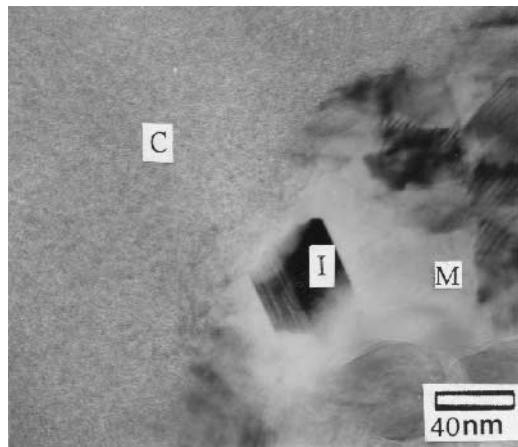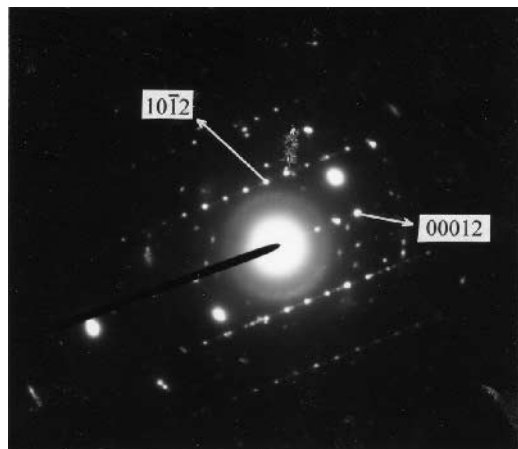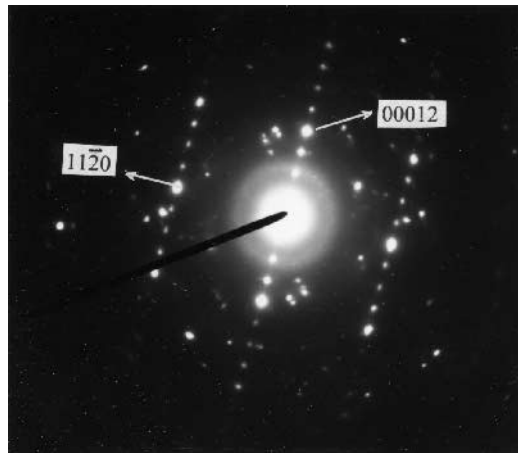

Fig. 1—Morphologies of carbon fibers with various conditions: (a) origin, (b) as-cast, (c) heat treatment at 600 °C for 36 h, and (d) heat treatment for 60 h.

(a)

(b)

(c)

Fig. 2—Fiber/matrix interface in the as-cast composite: (*a*) bright-field electron micrograph, SAD patterns from the aluminum carbide interface regions showing superpositions between carbide and aluminum matrix (*b*) with the zone axis [0110] and with the zone axis [1100] (M: Al matrix, C: carbon fiber, and I: interfacial product).
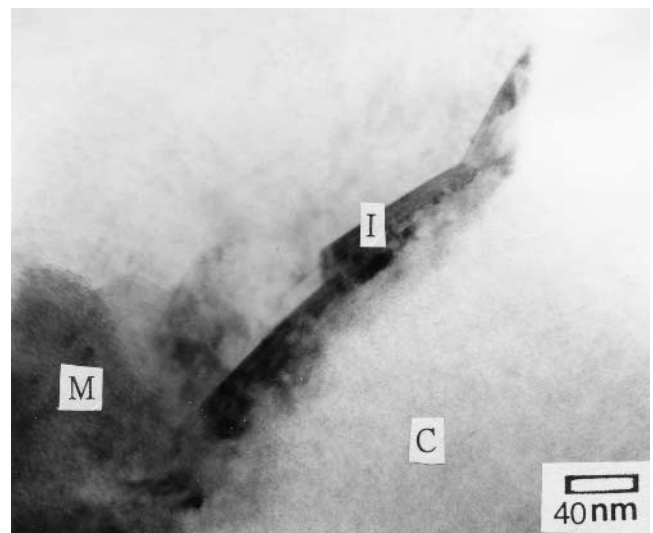
lattice parameters of $a = 0.333$ nm and $c = 2.4999$ nm in hexagonal coordinates. The TEM observation (Figure 3) also reveals lath-like crystals in the interfacial reaction zone of heat-treated composites. The small, slim crystals of Al_4C_3 in the specimens that had been treated for 12 hours had an
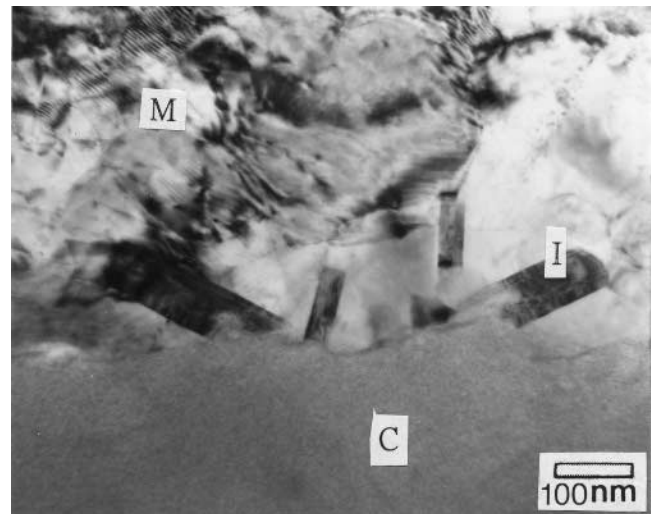
(a)
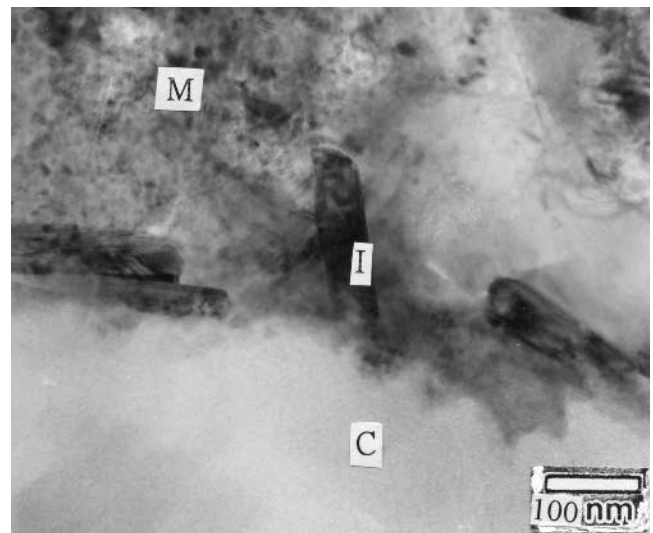
(b)

(c)

Fig. 3—TEM micrograph of fiber/matrix interface in heat-treated composites at 600 °C with (*a*) 12 h, (*b*) 36 h, and (*c*) 60 h.

average length of 150 nm and width of 50 nm. The aluminum carbide crystals were 200×60 nm for the composites heat treated for 60 hours. The fiber-matrix interface was examined by HRTEM to assess the growth of lath-like carbide. In Figure 4, HRTEM reveals that several platelets with the height of three fringes are observed on the upper side of the carbide crystal. This high-resolution electron micrograph shows that lattice fringes with a spacing of 0.83 nm lie parallel to the crystal axis. The lattice parameter of the Al_4C_3 parallel to the c-axis is three fringe spacings, or 2.49 nm.

C. *Electron Spectroscopy for Chemical Analysis*

Figure 5 displays an ESCA image of an original fiber. The ESCA spectrum of the C 1s line of carbon is observed at 284.5 eV, but the spectrum of the Al 2p line at 73 eV is not found. However, for the fiber surface of as-cast composites, the peak of Al 2p appears, as shown in Figure 6. The energy of the Al 2p level increases to 75.4 eV, corresponding to the formation of Al_4C_3, indicating that the aluminum carbide on the fiber surface of as-cast composites was formed. Figure 7 presents the results for composites after heat treatment. The energy of the Al 2p level is maintained at 75.4 eV, while the peak intensity increases with the duration of heat treatment.

D. *Tensile Properties*

Figure 8 plots the stress-strain curves of composites heat treated for various periods at 600 °C. Sudden failure occurred at 173 MPa under a strain of 5.08 pct for the as-cast composite shown in Figure 8(a). The stress-strain curves of heat-treated samples exhibit the same trend, *i.e.*, increasing
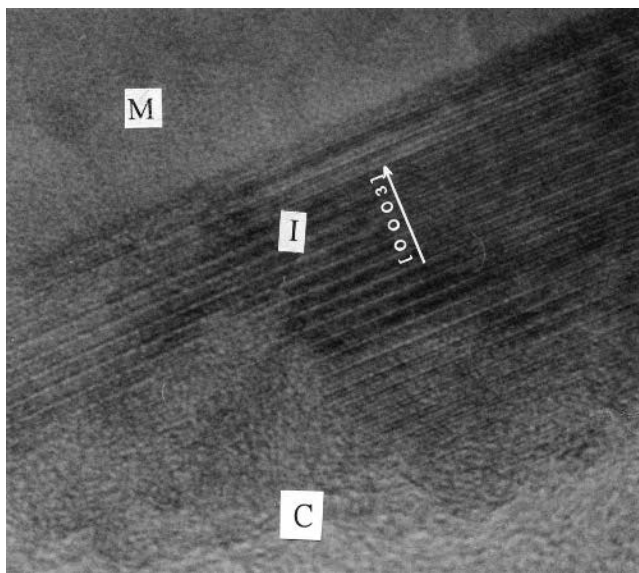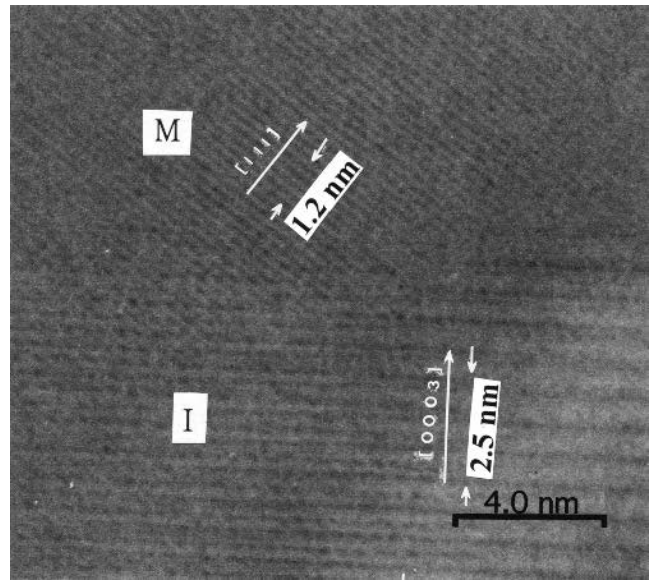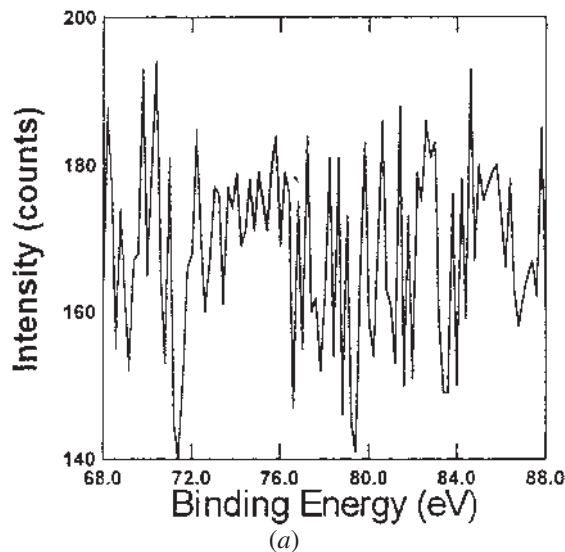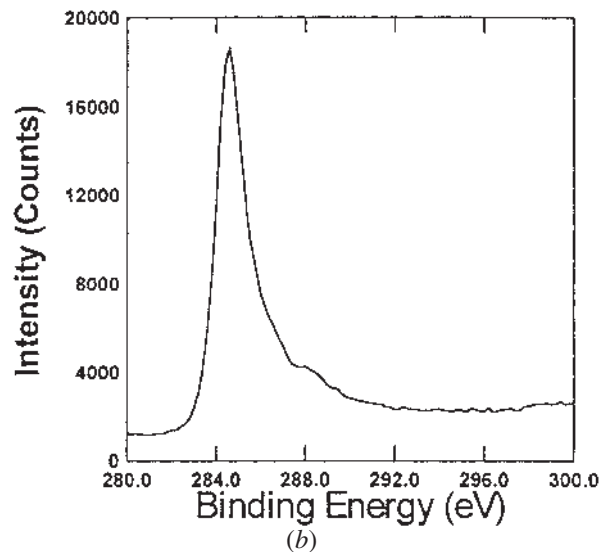

Fig. 4—(*a*) High-resolution electron micrograph of Al_4C_3 showing several plates with a height of three-fringe spacing on the upper side of the lath-like carbide. (*b*) Enlarged area of part (a).
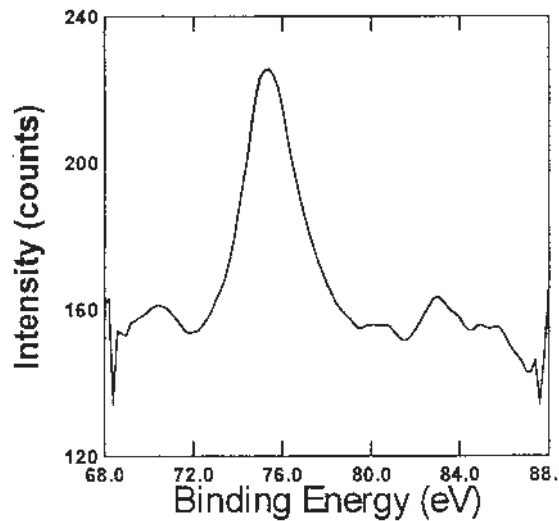

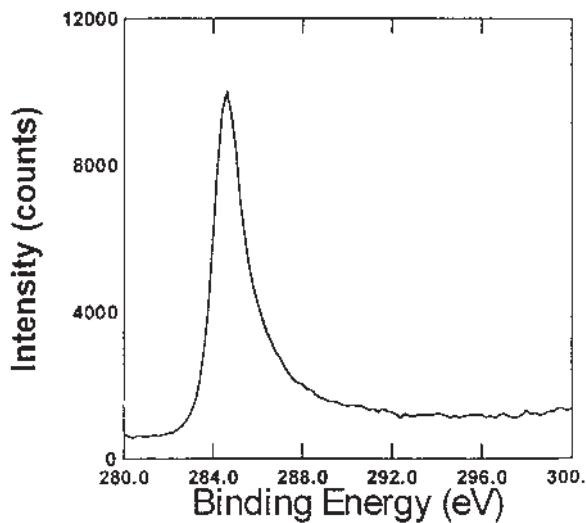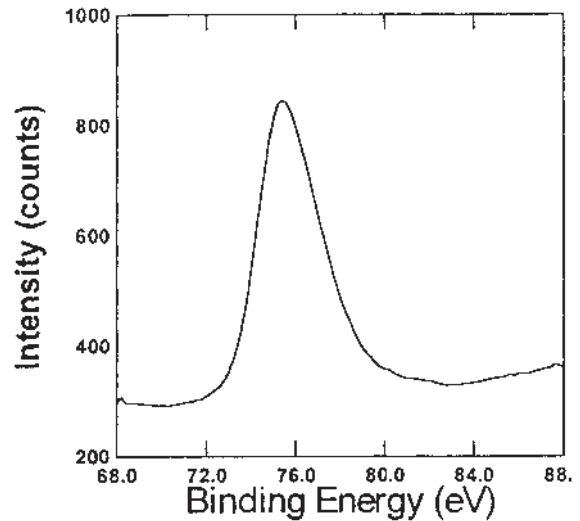Fig. 5—ESCA spectra of (*a*) Al 2p and (*b*) C1s from the original fibers.

Fig. 6—ESCA spectra of (*a*) Al 2p and (*b*) C1s from the fiber of as-cast composites.

Fig. 7—ESCA spectra of (*a*) Al 2p and (*b*) C1s from the fiber of the heat-treated composites at 600 °C for 60 h.
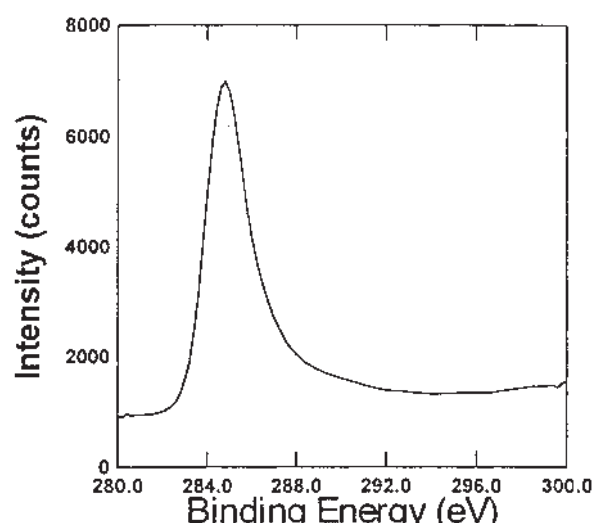
the amount of brittle carbides weakened the strength and elongation of the composites with time. Figure 9 plots the tensile stress and strain *vs* period of heat treatment. Both stress and strain decrease as the heat-treatment time increases.

IV. DISCUSSION

The present results clearly indicate that a chemical reaction between aluminum and carbon fibers has taken place during the liquid metal infiltration process. The products were confirmed to be rhombohedral aluminum carbide, of the type Al_4C_3. The carbide in Figure 2 was observed to nucleate heterogeneously from the fiber and to grow toward the aluminum matrix in the as-cast composites. Figure 3 presents the lath-like carbide crystals found in the heat-treated composites. The morphologies of carbides at the fiber surface (thickness/width ratios) did not appear to change with the duration of heat treatment. The lath-like crystals were

approximately 150-nm long and 50-nm wide after heat treatment for 12 hours. Each lath-like crystal was about 200-nm long and 60-nm wide after 60 hours. Aluminum carbide grew anisotropically. It was faster along the *a*- and *b*-axes of the basal plane than along the *c*-axis. However, no orientation relationship existed between the carbide and the aluminum matrix, although Yang *et al.*[23] found a relationship of the following form:

$$(0003) \ Al_4C_3 \ // \ (111) \ Al$$
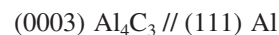
The amount of aluminum carbide was determined from ESCA spectra to determine how much aluminum carbide formed during heat treatment. The bonding energies for the $2_{p1/2}$ line of standard Al, and their compounds, were obtained from a variety of sources. The Al 2p peak (75.4 eV) was observed in as-cast composites and the heat-treated samples shown in Figures 6(a) and 7(a), indicating that aluminum carbide had been formed on the surface. Otherwise, the C 1s peak (284.8 eV) was observed in all ESCA spectra,
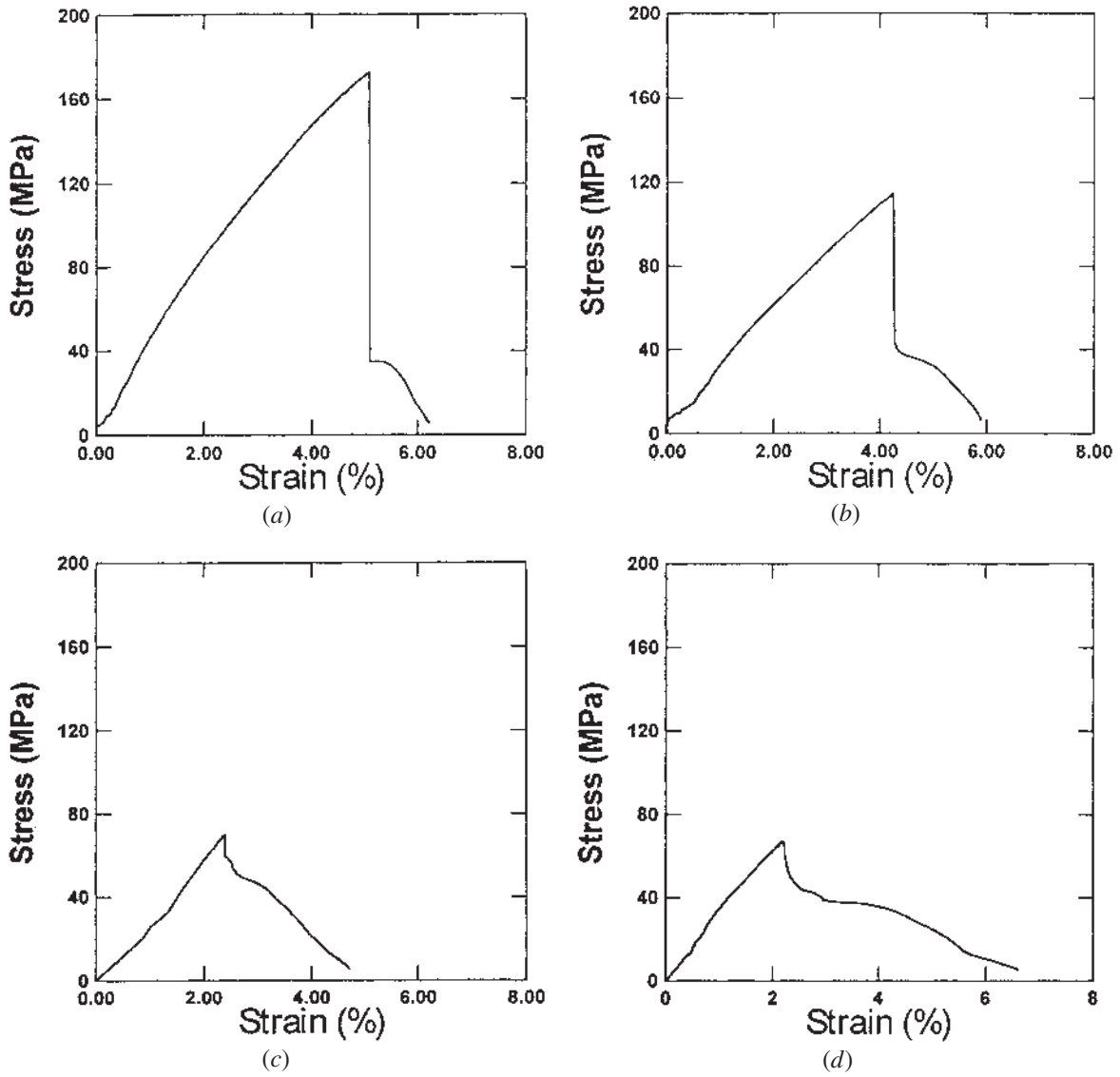
Fig. 8—The stress-strain curves of composites with various heat-treated time at 600 °C: (*a*) as-cast, (*b*) 12 h, (*c*) 36 h, and (*d*) 60 h.
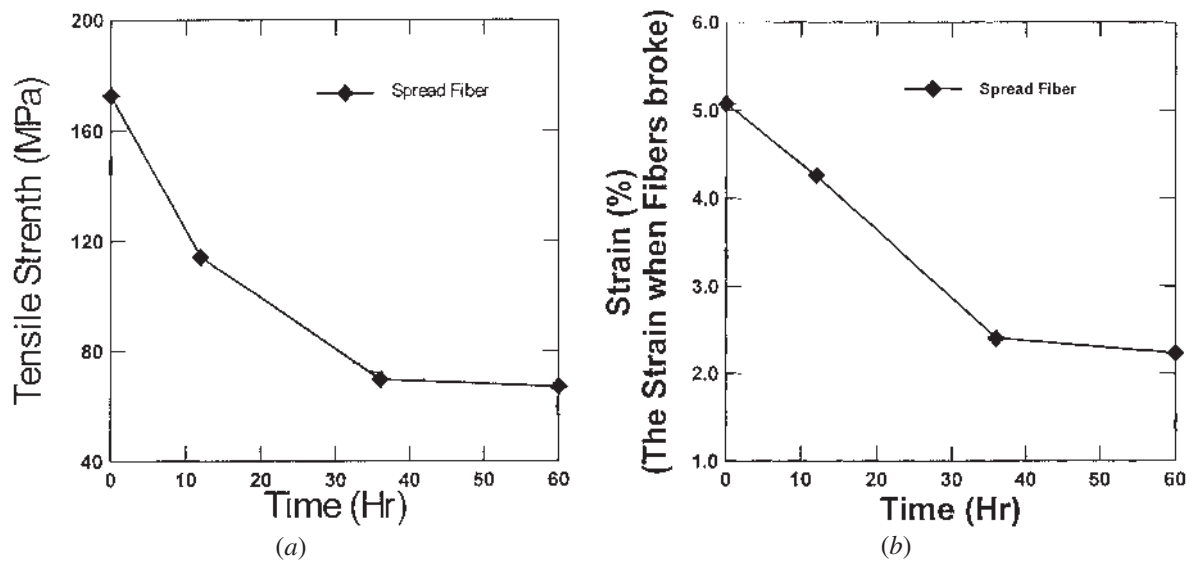

Fig. 9—The relationship between heat-treated time and (*a*) stress and (*b*) strain.

but the peak of carbon in Al_4C_3 was not revealed by ESCA. Arguably, the amount of Al_4C_3 may have been too little, in comparison with C 1s, to be detected. The area under the C 1s peak in Figure 6(b) represents the amount of unreacted carbon (A_c^u). The product Al_4C_3 is assumed to be unique. The peak area represents the amount of Al 2p in Figure 6(a). Given the chemical structure (Al_4C_3), the area under the Al 2p peak times 0.75 should equal the area under the C peak of the reacted carbon (A_c^r). Figure 10 plots the relationship between the period of heat treatment and the percentage of reacted carbon ($A_c^r/(A_c^r + A_c^u)$). Clearly, the amount of product (Al_4C_3) increases with time. However, the amount of Al_4C_3 increases more quickly after 36 hours. The result is consistent with the morphologies of the interface in Figure 1.

According to Kim et al.[25] the stress-strain relationship obtained by a fiber pull-out test can be divided into three kinds of debond processes: (1) totally unstable, (2) partially stable, and (3) totally stable. The results in Figure 8 correspond to the totally unstable debond processes. The stress-strain curve shows a monotonic increase in stress until debonding, followed by an instantaneous drop in load. The linear increase in stress represents primarily the transfer of frictional shear stress across the interface without virtual debonding, until the fibers break. The tensile strength
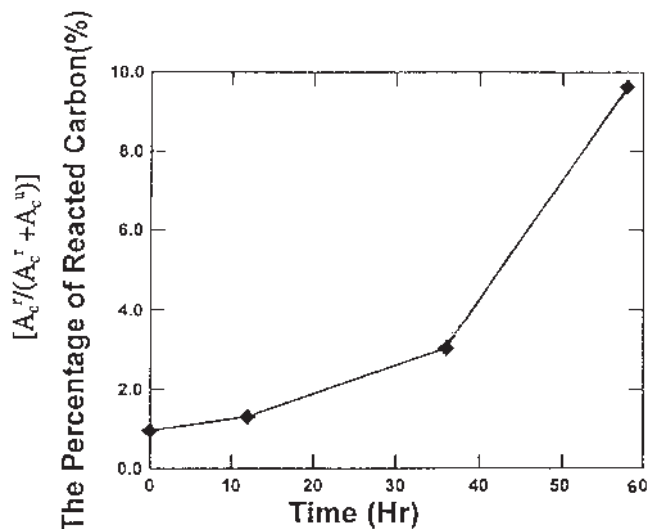
agrees with the values predicted by the simple rule of mixtures,[26]

$$\sigma_c = \sigma_m V_m + \delta \, \sigma_f V_f$$

where σ_c, σ_f, and σ_m represent the longitudinal strengths of the composite, fiber, and matrix, respectively; and δ is the efficiency of transfer of the strength of the fiber. Table I shows the results of the tensile tests on CF/Al composites and the efficiency of the transfer of fiber strength. The fibers withstood less stress as the value of δ decreased. The ultimate tensile stress and initial strain of the fibers decreased as the period of heat treatment increased. Figures 8 and 9 clearly show that the tensile strength and elongation of CF/Al composites decreased as the amount of Al_4C_3 increased. The product (Al_4C_3) formed at the CF/Al interface and protruded into the aluminum matrix. Figure 11 shows the fracture surface of the as-cast composite. The flat fracture surface with no fiber pull-out revealed a strongly bonded interface in this composite. Plastic deformation of the matrix may absorb part of the fracture energy and hinder the propagation of cracks in Figure 11(b). A large amount of brittle product may produce destructive notches on the surface of the fiber. They were crack initiated, resulting in the embrittlement of the surrounding aluminum matrix. Figure 12 depicts the cracks that formed at the interface and reveals that the matrix was barely plastically deformed.

V. CONCLUSIONS

Carbon-fiber-reinforced aluminum-matrix composites were prepared by spreading fibers and squeeze casting. The effects of the CF/Al interface effects on the strength of the composite and the fracture morphology were investigated. The main results are as follows:

1. The carbon fiber interacted with the aluminum matrix during fabrication as the aluminum carbide nucleated heterogeneously from carbon fibers and grew toward the aluminum matrix to form a lath-like crystal after heat treatment.
2. The growth of aluminum carbide was anisotropic, since it was faster along the *a*- and *b*-axes of the basal plane than along the *c*-axis.
3. Increasing the amount of brittle carbides after heat treatment weakened the strength and elongation of the composites with time.

Fig. 10—The relationship between heat-treated time and percentage of reacted carbon.

Table I. Mechanical Properties of Pure Aluminum and Composites

| Mechanical Properties Specimens	UTS (MPa)	Elongation (Pct)	Elongation of Initial Fiber Broken (Pct)	Transferred Efficiency of Fiber Strength δ (Pct)
Pure aluminum	45	28	—	—
As-cast composite	172.8	6.2	5.08	32.5
Heat-treated composite for 12 h	114.3	5.9	4.26	18.3
Heat-treated composite for 36 h	69.9	4.7	2.40	7.6
Heat-treated composite for 60 h	67.2	6.6	2.03	6.9
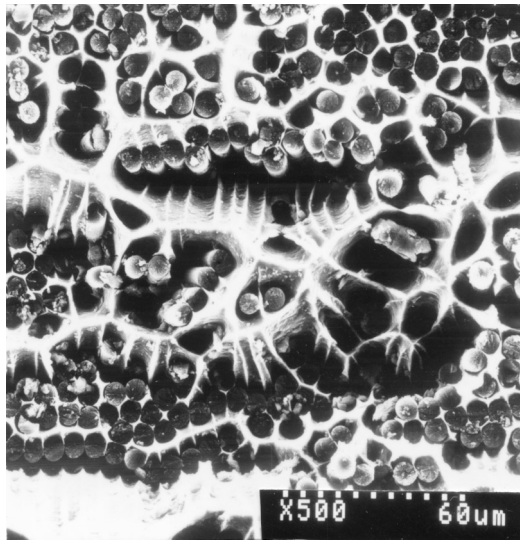
(a)
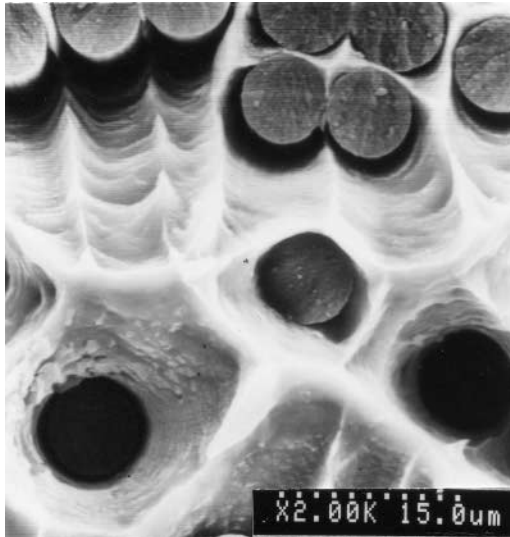
(b)

Fig. 11—(a) Fracture surface of the as-cast composite and (b) enlarge the area of part (a).
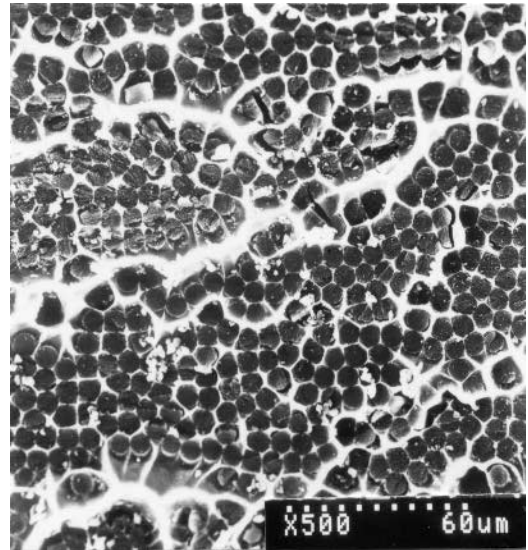
(a)
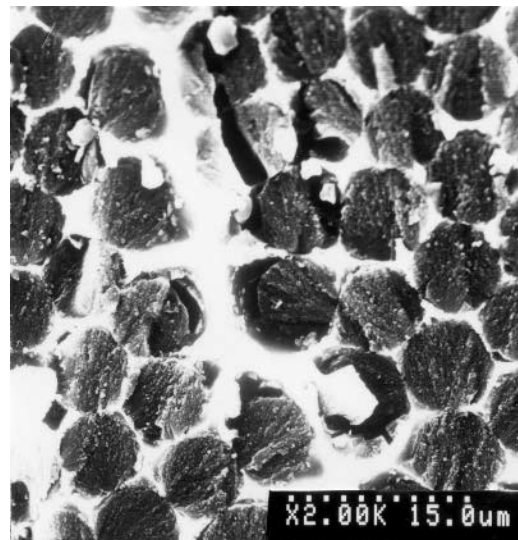
(b)

Fig. 12—(a) Fracture surface of the eat-treated composite at 600 °C for 12 h and (b) enlarge the area of part (a).

REFERENCES

1. F. Delannay, L. Foryen, and A. Deruyttere: *J. Mater. Sci.*, 1987, vol. 22, pp. 1-16.
2. R.V. Subramanian and A. Nyberg: *J. Mater. Res.*, 1992, vol. 7(3), pp. 677-88.
3. Li-Min Zhou, Yiu-Wing-Mai, and Caroline Baillie: *J. Mater. Sci.*, 1994, vol. 29, pp. 5541-50.
4. Sunil G. Warrier and Ray Y. Lin: *Scripta Metall. Mater.*, 1993, vol. 29, pp. 1513-18.
5. Zhenhia Xia, Yaohe Zhou, Zhiying Mao, and Baolu Shang: *Metall. Trans. B*, 1992, vol. 23B, pp. 295-302.
6. R. Asthana: *J. Mater. Sci.*, 1998, vol. 33, pp. 1959-80.
7. G. Leonhardt, E. Kieselstein, H. Podlesak, E. Than, and A. Hofman: *Mater. Sci. Eng.*, 1991, vol. A135, pp. 157-60.
8. Andreas Mortensen: *Mater. Sci. Eng.*, 1991, vol. A135, pp. 1-11.
9. J.K. Yu, H.L. Li, and B.L. Shang: *J. Mater. Sci.*, 1994, vol. 29, pp. 2641-47.
10. D. Huda, M.A. El Baradie and M.S.J. Hashmi: *J. Mater. Processing Technol.*, 1993, vol. 37, pp. 529-41.
11. Feng Wu and Jing Zhu: *Composites Sci. Technol.*, 1997, vol. 57, pp. 661-67.
12. R. Wu: *Proc. 2nd Int. Conf. on Composite Interfaces*, (ICCI-II) held June 13–17, 1988, in Cleveland, Ohio, USA/editor, Matsuo Ishida, p. 43.
13. H. Nayeb-Hashemi and J. Seyyedi: *Metall. Trans. A*, 1989, p. 381.
14. M.F. Amateau: *J. Compos. Mater.*, 1976, vol. 20A, p. 274.
15. I.H. Khan: *Metall. Trans. A*, 1976, vol. 10, p. 1281.
16. G. Blankenburgs: *J. Aus. Inst. Met.*, vol. 7A, 1969, p. 236.
17. W.C. Harrigan, Jr.: *Metall. Trans. A*, 1978, vol. 9A, p. 503.
18. H.S. Yoon and A. Okura: *SAMPE J.*, 1990, vol. 26, p. 19.
19. R.T. Pepper and R.A. Penty: *J. Composite Mater.*, 1974, vol. 8, pp. 29-37.
20. L. Xiangun and Z. Hanlin: Proc. 5th Int. Conf. on Composite Materials, ICCM-V, in San Diego, California, W.C. Harrigan, Jr. *et al.*, eds., AIME, 1985, pp. 623-29.
21. S.J. Baker and W. Bonfield: *J. Mater. Sci.*, 1978, vol. 13, p. 1329.
22. A. Okura and H. Asanuma: *Compos. Sci. Eng.*, 1985, vol. 24, p. 243.
23. H. Yang, M. Gu, W. Jiang, and G. Zhang: *J. Mater. Sci.*, 1996, vol. 31, pp. 1903-07.
24. J.C. Chen and C.G. Chao: *Metall. Mater. Trans. B*, 2001, vol. 32B, pp. 329-39.
25. K.J. Kim, C. Baillie, and Y.W. Kai: *J. Mater. Sci.*, 1991, vol. 22, pp. 445-47.
26. M.A. Meyers and K.K. Chawla: *Mechanical Metallurgy—Principle and Applications*, Prentice-Hall, Inc., 1984, p. 445.